Surface atomic structures of Fe_2O_3 nanoparticles coated with cetyltrimethyl ammonium bromide and sodium dodecyl benzene sulphonate: an extended x-ray absorption fine-structure study

1999 J. Phys.: Condens. Matter 11 4961

(http://iopscience.iop.org/0953-8984/11/26/301)

J. Phys.: Condens. Matter **11** (1999) 4961–4970. Printed in the UK PII: S0953-8984(99)00812-7

Surface atomic structures of Fe_2O_3 nanoparticles coated with cetyltrimethyl ammonium bromide and sodium dodecyl benzene sulphonate: an extended x-ray absorption fine-structure study

Wu Zhonghua†, Guo Lin†, Li Qianshu‡ and Zhu Hesun‡

† Beijing Synchrotron Radiation Laboratory, Institute of High Energy Physics, Chinese Academy of Sciences, PO Box 918, Bin 2-7, Beijing 100039, People's Republic of China
‡ College of Chemical Engineering and Materials Science, Beijing Institute of Technology, PO Box 327, Beijing 100081, People's Republic of China

E-mail: wuzh@bepc3.ihep.ac.cn

Received 11 January 1999, in final form 14 May 1999

Abstract. Fe_2O_3 nanoparticles coated with sodium dodecyl benzene sulphonate (DBS) or cetyltrimethyl ammonium bromide (CTAB) were prepared by using a microemulsion method in the system water/toluene. The nanoparticles were characterized by means of transmission electron microscopy and average particle sizes of 5.0 nm and 6.0 nm were found for DBS-modified and CTAB-modified nanoparticles respectively. The local atomic structures of these iron(III) oxide nanoparticles were probed by using the extended x-ray absorption fine-structure technique. Fe K absorption spectra were collected at beam line 4W1B of Beijing Synchrotron Radiation Facility. A structural model was proposed for describing their atomic structures. The Fe–O bond length at the surface of DBS-coated Fe_2O_3 nanoparticles was found to be similar to that in bulk Fe_2O_3, but there was about 0.04 Å expansion for the CTAB-coated Fe_2O_3 nanoparticles. On the basis of the model proposed in this paper, the thicknesses of the surface layers were estimated to be 0.5 nm and 0.7 nm, respectively, for the DBS-coated and CTAB-coated Fe_2O_3 nanoparticles. The anharmonicity of the atomic vibration and the asymmetry of atom-pair distribution were found to be larger at the surface of the nanoparticles than in the bulk material, while the Debye–Waller factors are almost the same for the surface and the core parts of the nanoparticles. It can be concluded that the atomic structure of the nanoparticle surface is ordered, but the atom-pair distribution is asymmetric.

1. Introduction

Recently, there has been great scientific interest in the synthesis of Fe_2O_3 nanoparticles and modifications of their size, morphology, and properties for different applications in anticorrosion protective paints, magnetic oxide ceramics, and gas sensors, as well as in fundamental research in colloid and surface chemistry [1–3], microstructure [4–6], and nonlinear optical properties [7]. All of the peculiar properties of nanometre-sized material are due to their high ratio of surface to volume and to quantum-size effects [8, 9]. Usually, nanometre-sized materials are thought to consist of two components, i.e. the core part and the surface or interface part. Although gas-like, order, and order–disorder models have been proposed for describing the atomic structures of the surfaces and interfaces of nanometre-sized materials, structural models of surfaces and interfaces of nanoparticles are still worthy of

0953-8984/99/264961+10$19.50

investigation. Especially for nanoparticles modified by surfactant, the surfactant's influence on the surface atomic structure of the nanoparticles is not clear.

The extended x-ray absorption fine-structure (EXAFS) technique is a powerful tool for probing the local atomic structures because of its element specificity and independence of the long-range order of materials. In this paper, two types of Fe_2O_3 nanoparticle, coated with sodium dodecyl benzene sulphonate (DBS) and coated with cetyltrimethyl ammonium bromide (CTAB), were prepared. Using the EXAFS technique, we probed the local atomic structures at the surfaces of the nanoparticles and compared the influences of different surfactants on the surface structures. We expect this to prove helpful for explaining the peculiar properties of these nanoparticles.

2. Experimental procedure

2.1. Sample preparation

Fe_2O_3 nanoparticles have been prepared by different methods [10, 11]. In this paper, Fe_2O_3 nanoparticles coated with DBS and CTAB were prepared using microemulsion methods in the system water/toluene. All of the chemicals and reagents used were of analytical grade. The $FeCl_3{\cdot}6H_2O$, NaOH, and benzene were obtained from Beijing Reagent Corporation and used as received, without further purification. The synthesis process is as follows:

(1) *DBS-coated Fe_2O_3 nanoparticles*: 25 ml of 0.1 M aqueous $FeCl_3$ and 160 ml of toluene were poured into a beaker. We stirred the mixture and then added a certain volume of DBS ($C_{12}H_{25}$–C_6H_{10}–SO_3^- + Na^+) as a surfactant. After that, 70 ml of 0.1 mol l^{-1} aqueous NaOH was stirred into the solution. Finally this mixture was allowed to stand for 6 h, and it formed two layers. The upper layer is a reddish-brown transparent organic sol. The lower layer is a colourless aqueous solution.

In the upper layer, the surfactant forms the microreactor in which the iron oxide nucleates and grows to form the nanoparticles. At the interface between the nanoparticle and the surfactant DBS, there is probably chemical bonding between Fe^{3+} and the $C_{12}H_{25}$–C_6H_{10}–SO_3 group. The remaining irons (as iron oxide precipitate) and the Na^+ locate in the lower layer.

Taking the upper reddish-brown transparent organic sol, the nanometre Fe_2O_3 powder was obtained by removing the solvent from it; further heat treatment was carried out at 400 °C for 1 h under the protection of a N_2 atmosphere.

(2) *CTAB-coated Fe_2O_3 nanoparticles*: 2 g of CTAB ($C_{16}H_{33}$–$(CH_3)_3$–N^+ + Br^-) was dissolved into a mixture of 240 ml of chloroform ($CHCl_3$) and 160 ml of *n*-ethyl carbinol ($CH_3(CH_2)_2OH$). This solution was stirred for 30 minutes and became transparent. Then it was divided into two parts. A certain volume of 0.1 mol l^{-1} aqueous $FeCl_3$ was added to one part, while 0.1 mol l^{-1} aqueous NaOH was added to the other. We stirred the two mixtures until they became transparent solutions. After that the two solutions were mixed by means of ultrasonic waves and stirred for 1 h. A similar procedure was performed to that in the preparation of DBS-coated nanoparticles. At the interface between the nanoparticles and the surfactant CTAB, there is probably bonding between the O^{2-} and the $C_{16}H_{33}$–$(CH_3)_3$–N^+ group. The Br^- and the remaining iron oxide precipitate were deposited in the aqueous solution.

The organic sol was dried by rotatory evaporation. Next it was dissolved into the toluene; this formed a reddish-brown transparent solution. The nanometre Fe_2O_3 powder was obtained from this solution by removing the solvent from the organosol, and was heat treated at 400 °C for 1 h under the protection of a N_2 atmosphere.

We believe that the bonding between the surfactant DBS or CTAB and the Fe_2O_3 nanoparticles will increase the thermal stability of the surfactants. We assume here that the surfactants CTAB and DBS are also thermally stable at 400 °C. While the thermal treatment at 400 °C probably leads to partial separation of the hydrocarbon chain from the head group, the head groups bonded to the nanoparticles may still form a covering layer coating the nanoparticles.

2.2. TEM characterization

The samples were characterized using a transmission electron microscope (TEM, H-8000, Japan) which was operated at 200 kV. The TEM images and electron diffraction patterns of the samples are presented as figure 1. The average particle sizes were found to be 5.0 nm and 6.0 nm for the Fe_2O_3 nanoparticles modified by DBS and CTAB, respectively. The interplanar spacing d of the ferric oxides in the composite particles can be calculated from the electron diffraction pattern. The data together with those [12] for bulk α-Fe_2O_3 are listed in table 1.

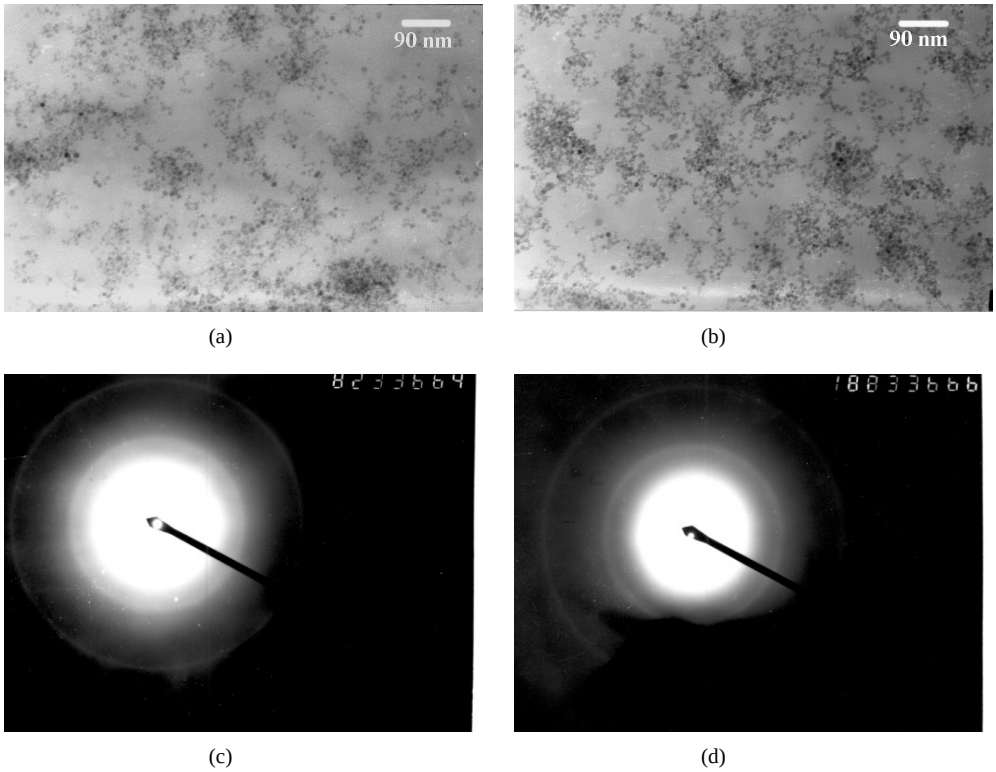

Figure 1. (a) A transmission electron microscope image of DBS-coated Fe_2O_3 nanoparticles. The average particle size is about 5.0 nm. (b) A transmission electron microscope image of CTAB-coated Fe_2O_3 nanoparticles. The average particle size is about 6.0 nm. (c) A selected-area electron diffraction pattern of DBS-coated Fe_2O_3 nanoparticles. The diffraction rings can be indexed with reference to α-Fe_2O_3. (d) A selected-area electron diffraction pattern of CTAB-coated Fe_2O_3 nanoparticles. The diffraction rings can be indexed with reference to α-Fe_2O_3.

Table 1. Interplanar spacings (in Å) of DBS-coated and CTAB-coated Fe_2O_3 nanoparticles as well as the reference data (reference [12]) for bulk α-Fe_2O_3.

Diffraction ring	d_{calc} (for DBS)	d_{calc} (for CTAB)	d (for bulk α-Fe_2O_3)
1	2.297	2.310	2.292
2	1.326	1.347	1.312
3	1.147	1.159	1.141

2.3. EXAFS spectra collection

EXAFS spectra were collected at the EXAFS station (beam line 4W1B) of Beijing Synchrotron Radiation Laboratory. The nanoparticles were homogeneously smeared on Scotch tape®. More than eight layers were folded to reach the optimum absorption thickness ($\Delta\mu\, d \approx 1.0$, where d is the physical thickness of the sample). X-ray absorption spectra of the Fe K edge for bulk Fe_2O_3 and for nano-Fe_2O_3 coated with CTAB and DBS were collected at ambient temperature in the transmission mode. The storage ring was run at 2.2 GeV with an electron current of about 50 mA. High harmonics were eliminated by detuning the double-crystal Si(111) monochromator, with about 40% decrease in the fundamental wave intensity. The incidence and transmission x-ray intensities were, respectively, detected by ion chambers that were installed in front of and behind the sample. The x-ray energy was calibrated by using the inflection point of the Cu K absorption edge (8980.3 eV). The energy resolution at the Fe K absorption edge is about 2 eV. The absorption spectra were collected from 200 eV below the absorption threshold to over 1000 eV above the threshold. The collection time for each datum point was one second.

3. EXAFS data analysis

The EXAFS data were analysed by using a common data-analysis method [13]. The mid-point of the absorption jump was chosen as the energy threshold (7112 eV). The pre-edge absorption background was fitted and subtracted by using the Victoreen formula. The post-edge absorption backgrounds were fitted by using the spline function and subtracted from the absorption spectra. The EXAFS functions were normalized by using the absorption edge jump and were Fourier transformed to R-space with k^3-weighing over the range 2.7 to 14.4 Å. Fourier filtering was performed over the range 0.9 to 2.1 Å. The Hanning window function [13] was used in the Fourier transforming and filtering process. The Fourier transform spectra and the nearest-neighbour-coordination EXAFS functions are, respectively, shown in figures 2 and 3.

For most low-temperature systems, symmetrical atom-pair distribution is adequate to describe the local atomic structures. However, for moderate and larger disorder and/or anharmonic systems, an asymmetrical atom-pair distribution is always necessary. In this study, we consider an asymmetrical distribution. The following EXAFS formula [14, 15] was used to fit the experimental spectra:

$$\chi_j(k) = \frac{s_0^2 N_j}{k R_j^2} F_j(\pi, k) \exp(-2k^2\, \Delta\sigma_j^2) \exp(-2R_j/\lambda_j) \sin(2kR_j + \phi_j + \Sigma_j) \tag{1}$$

where

$$\Sigma_j = -4\frac{\Delta\sigma_j^2}{R_j}k - \frac{4}{3}\sigma_j^{(3)}k^3. \tag{2}$$

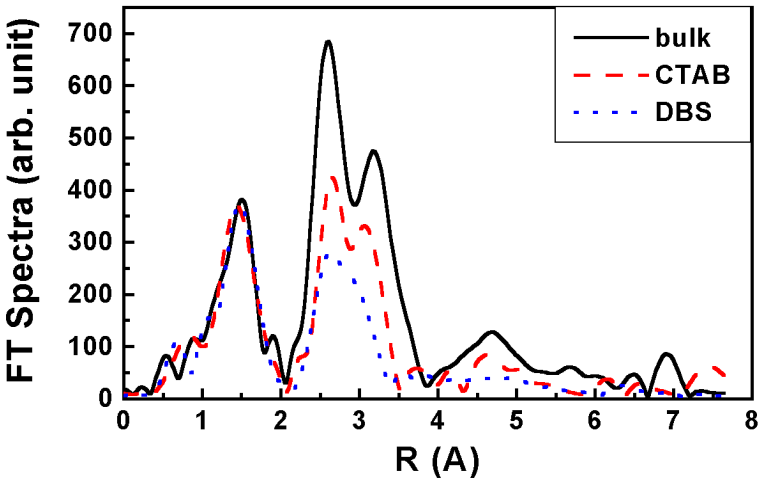

Figure 2. Fourier transform spectra of Fe K absorption in bulk α-Fe_2O_3 (solid curve), and DBS-coated (dotted curve) and CTAB-coated (dashed curve) Fe_2O_3 nanoparticles. The phase shifts of the central and backscattered atoms are not removed from the spectra.

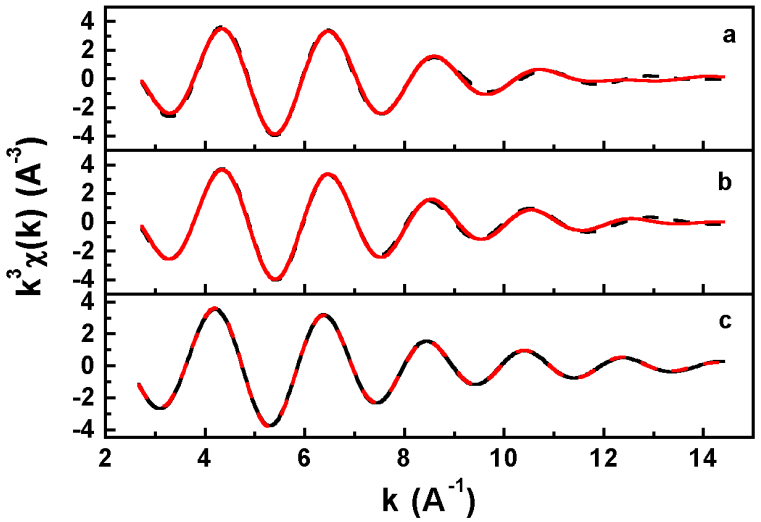

Figure 3. Experimental (dashed curve) and fitted (solid curve) EXAFS curves with k^3-weighting of the Fe–O coordination in: (a) CTAB-coated Fe_2O_3 nanoparticles; (b) DBS-coated Fe_2O_3 nanoparticles; and (c) bulk α-Fe_2O_3.

Here, Σ_j is the phase correction term for the asymmetrical distribution, $\sigma_j^{(3)}$ is the third cumulant, N_j is the number of backscattered atoms located at distance R_j away from the absorber, $F_j(\pi, k)$ is the backscattering factor, s_0^2 is the reduction factor, λ_j is the mean free path of the photoelectrons, ϕ_j is the phase shift, and $\Delta\sigma_j^2 = \sigma_{uj}^2 - \sigma_{sj}^2$, where σ_{uj}^2 and σ_{sj}^2 are, respectively, the Debye–Waller factors of the unknown and reference samples.

The backscattering amplitude

$$A_s(\pi, k) = s_0^2 F(\pi, k) \exp(-2k^2\sigma_s^2) \exp(-2R_s/\lambda_s)$$

and phase shift ϕ_s were extracted for the reference sample $LaFeO_3$ [16]. In view of the transferability of the backscattering amplitude and the phase shift, they were substituted for those of the unknown samples in equation (1). The fitting curves for the experimental EXAFS functions are also shown in figure 3. Table 2 tabulates the fitting parameters.

Table 2. Structural parameters of the Fe–O coordination in bulk Fe_2O_3 and nanometre Fe_2O_3 coated with CTAB and DBS. α and β are, respectively, the contents of the core part and the surface part. N is the oxygen coordination number of the iron atom. R is the length of the bond between the iron and oxygen. $\Delta\sigma^2$ and $\sigma^{(3)}$ are, respectively, the difference in Debye–Waller factor between the reference and the samples, and the third cumulant of the Fe–O atom-pair distribution. ΔE_0 is the shift of the energy threshold.

Fe_2O_3	α	β	N	R (Å)	$\Delta\sigma^2$ (Å^2)	$\sigma^{(3)}$ (Å^3)	ΔE_0 (eV)
Bulk[a]	1.0	0.0	3.0 ± 0.4	1.935 ± 0.010	0.0020 ± 0.0040	-0.000039 ± 0.00050	-0.80 ± 1.0
			3.0 ± 0.4	2.063 ± 0.010	0.0089 ± 0.0040	0.000317 ± 0.00050	-0.80 ± 1.0
CTAB[b]	0.44	0.56	5.2 ± 0.4	2.044 ± 0.010	0.0034 ± 0.0040	0.002107 ± 0.00050	6.9 ± 1.0
DBS[b]	0.52	0.48	6.0 ± 0.4	2.008 ± 0.010	0.0049 ± 0.0040	0.001180 ± 0.00050	5.9 ± 1.0

[a] Here 'bulk' stands for bulk α-Fe_2O_3.
[b] 'CTAB' and 'DBS' are, respectively, standing for CTAB- and DBS-coated Fe_2O_3 nanoparticles. Here only the parameters for the surface part are listed in the table. The parameters of the core part are the same as those listed for bulk α-Fe_2O_3.

4. Results and discussion

From the coordination peaks located in the region 2–4 Å, as shown in figure 3, it can be seen that the magnitudes of the coordination peaks have obviously decreased for the nanoparticles, comparing with the bulk material, especially for DBS-coated Fe_2O_3. Because these coordination peaks correspond to the contributions of the next-nearest-neighbour Fe atoms and O atoms, the diminution of such a peak indicates that the number of Fe atoms backscattered around the Fe centre has decreased. This is due to the larger ratio of surface to volume of the Fe_2O_3 nanoparticles; the Fe atoms located at the surfaces of the particles partially lose next-nearest-neighbour Fe atoms, which lowers the coordination peak. Fe_2O_3 nanoparticles coated with DBS have smaller average particle sizes and larger ratios of surface to volume than ones coated with CTAB, so the coordination peak is more reduced, as is apparent in the Fourier transform spectra. This decrease of the coordination peak is a common feature for nanoparticles. Because the next-nearest-neighbour coordination is quite complicated, several coordination shells of Fe–Fe and/or Fe–O are included within the region 2–4 Å. Further data analysis for this coordination peak is inappropriate.

In the data analysis of the first coordination peaks located at about 1.5 Å, crystalline $LaFeO_3$ was chosen as the reference sample. The backscattering amplitude and phase shift of the Fe–O bond were extracted for the following crystallographic data [16]: $N = 6$, $R = 2.006$ Å. In bulk α-Fe_2O_3, there are two subshells around the central Fe atom, all with three O atoms backscattered. The EXAFS spectrum of bulk α-Fe_2O_3 was fitted by using two shells; the structural parameters are listed in table 2. The nanoparticles of Fe_2O_3 have been identified as having structures similar to that of α-Fe_2O_3 from TEM results. Besides the CTAB or DBS covering layer, we suppose that these nanoparticles each consist of two parts, i.e., the core part (α) and the surface part (β). The core parts have the same atomic structures as bulk Fe_2O_3, while the surface parts are different and depend on the covering layer (CTAB or DBS). The

mixed-phase and mixed-coordination EXAFS formula [17] was used to fit the EXAFS spectra of the CTAB- and DBS-coated Fe_2O_3 nanoparticles. The structural parameters obtained for bulk Fe_2O_3 were chosen to describe the core parts; these parameters were fixed in the fitting except the coordination number N_1 ($=N_2$). An additional shell was used to describe the surface parts. Six parameters (the maximum number of parameters allowed is nine) were used in the fitting, i.e., the coordination number N_1 ($=N_2$) of the core part, the coordination number N_3, the bond length R_3, the Debye–Waller factor $\Delta\sigma^2$, the third cumulant $\sigma^{(3)}$, and the energy shift ΔE_0 of the surface shell. From the coordination number N_1 or N_2, the content of the core part (α) was obtained as $N_1/3$, and the content (β) of surface part was obtained as $1-\alpha$. The actual coordination number for the surface part was obtained as $N_s = N_3/\beta$. The parameters obtained for CTAB- and DBS-coated Fe_2O_3 nanoparticles are listed in table 2.

From table 2, the average Fe–O bond length in the core part or in the bulk Fe_2O_3 can be calculated to be 1.999 Å. The average Fe–O bond lengths in CTAB-coated and DBS-coated nano-Fe_2O_3 are, respectively, 2.023 and 2.003 Å. This is consistent with the TEM results. For DBS-coated Fe_2O_3 nanoparticles, the Fe–O bond length (2.008 Å) of the surface part is only slightly larger than that (1.999 Å) in the core part, while for the CTAB-coated Fe_2O_3 nanoparticles, the Fe–O bond length (2.044 Å) of the surface part is obviously larger. This implies that the CTAB surfactant strongly pulls the O atoms on the surface/interface nearer to itself. Although the Debye–Waller factors for the nanoparticles show no obvious change from those corresponding to bulk Fe_2O_3, the third cumulants are dramatically increased for the surface parts. This demonstrates that the nearest-neighbour atomic structures at the surfaces and interfaces of the nanoparticles are quite ordered, but the atomic vibrations are seriously suppressed by the surfactant, and this leads to the large anharmonicity. Comparing the surfactants CTAB and DBS, we found that CTAB has more influence than DBS on the surface atomic structures. This can be summarized as follows. Firstly, CTAB has more spatial resistance than DBS and produces more distortion and holes in the interface between Fe_2O_3 and the CTAB. Secondly, CTAB is a cation-ligand surfactant, while DBS is an anion-ligand surfactant. The former tends to attract O anions and the latter tends to attract Fe cations. Usually, the outermost shells of the Fe_2O_3 nanoparticles in air are occupied by the oxygen atoms. As regards the surface parts of the nanoparticles, the average coordination number for O around Fe in DBS-coated Fe_2O_3 tends to retain the same value as for bulk α-Fe_2O_3, while it appears to slightly decrease for CTAB-coated Fe_2O_3. This can be explained as follows. The cation surfactant CTAB attracts the O atoms and leaves O vacancies in the interface, which results in a decrease of the O coordination number. But the anion surfactant DBS repels the O atoms and compensates for the O vacancies.

Figure 4 shows a map of the surfactant, the surface component, and the core part, for the DBS- and CTAB-coated Fe_2O_3 nanoparticles. For the crystalline Fe_2O_3 nanoparticles, the core part is relatively stable and retains the structure of the bulk material, while the surface part shows more anharmonicity. In this study, about 44% of the atoms are located in the core part while 56% of the atoms are located in the surface part for the CTAB-coated ($\sim$6 nm) Fe_2O_3 nanoparticles. The contents of the core part and the surface part are, respectively, about 52% and 48% for the DBS-coated ($\sim$5 nm) Fe_2O_3 nanoparticles.

We assume the nanoparticles to be spherical. The thickness of the surface part of the CTAB-coated Fe_2O_3 nanoparticles is about 0.7 nm while that of the surface part of the DBS-coated Fe_2O_3 nanoparticles is about 0.5 nm.

In fact, in this study, the contents of the core part (α) and the surface part (β), which were derived from the EXAFS results, are independent of the shape of the particles. However, the estimate of the thickness (δ) of the surface layer depends on the shape of the particles. The

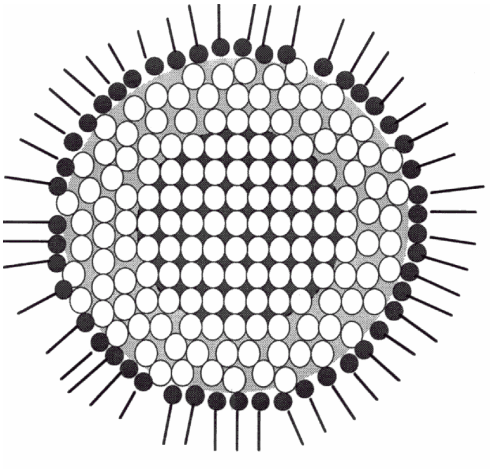

Figure 4. A map showing the surfactant, the surface component, and the core part for the DBS-coated and CTAB-coated Fe_2O_3 nanoparticles.

ratios (α) of the core partial volume V_c (assuming a thickness δ of the surface layer) to the total volume V are given below for particles with different shapes. For cubes and spheres,

$$\alpha = (1-\gamma)^3 \qquad \gamma = 2\delta/D$$

where D is the edge length of the cubes or the diameter of the spheres. For cuboids and ellipsoids,

$$\alpha = (1-\gamma_x)(1-\gamma_y)(1-\gamma_z)$$
$$\gamma_x = 2\delta/D_x \qquad \gamma_y = 2\delta/D_y \qquad \gamma_z = 2\delta/D_z$$

where D_x, D_y, D_z are the edge lengths of the cuboids or the three diameters of the ellipsoids. For cylinders,

$$\alpha = (1-\gamma_{xy})^2(1-\gamma_z)$$
$$\gamma_{xy} = 2\delta/D_{xy} \qquad \gamma_z = 2\delta/L_z$$

where D_{xy} is the diameter of the bottom of the cylinder and L_z is the length of the cylinder. For cases which obviously diverge from cubes or spheres—for example, where $D_x = 4$ nm, $D_y = 6$ nm, $D_z = 8$ nm—we estimate the thickness of the surface layer to be 0.65 nm. This value is about 0.07 nm smaller than that estimated for a sphere with a 6.0 nm diameter. Similarly, for $D_x = 3$ nm, $D_y = 5$ nm, $D_z = 7$ nm, a thickness of 0.43 nm can be obtained for the surface layer. This is about 0.06 nm less than those for the spheres or cubes with diameters of 5.0 nm. From the above discussion, we know that, for a certain volume of particles at certain fixed contents of the core part and the surface part, the thickness of the surface layer estimated using the sphere or cube model is the maximum, comparing with the values estimated using other shapes. Evidently, if the dimensions in the three directions are not obviously different, the estimated thickness of the surface layer should be approximately the same for different shapes of particle. Then, using the sphere model to estimate the thickness of the surface layer is adequate.

Generally speaking, there are two sources of uncertainty in the fitting parameters. One is the experimental errors, including the statistical error and the systematic error in the EXAFS spectrum collections. The other arises from the procedure of data analysis, including the

selection of a fitting model and the selection of the parameters used in the background removal, Fourier transformation, window filtering, etc. Most of these uncertainties were suppressed well by the careful experimental preparation and data analysis. The uncertainties of the fitting parameters were evaluated according to the standards and criteria of [18], and are given in table 2. As for the uncertainty of the thickness of the surface layer, it is mainly attributable to the uncertainty in the coordination number and how near to spherical the shape of the nanoparticles is. The uncertainty in the thickness of the surface layer was estimated to be about 0.1 nm.

The anharmonicity of the atomic vibration in these nanoparticles gradually increases from the core to the surface. The EXAFS technique gives us an averaged result. From this study, we recognize that the surfaces and interfaces of nanoparticles coated with surfactant are quite ordered, but the anharmonicity of the atomic vibration increases dramatically.

5. Conclusions

We studied the local atomic structures of Fe_2O_3 nanoparticles coated with the surfactants CTAB and DBS. Each nanoparticle consists of two parts, i.e. a core part and a surface part. The surface parts are quite ordered but with larger anharmonicity. The contents of the surface parts approach 50% for the 5 or 6 nm Fe_2O_3 nanoparticles. The surface thickness is, respectively, about 0.7 nm and 0.5 nm for the 6 nm CTAB-coated Fe_2O_3 particles and the 5 nm DBS-coated Fe_2O_3 ones. The bond length of the Fe–O pair is almost the same, equal to 2.008 Å, for the surface parts of DBS-coated Fe_2O_3 nanoparticles and the bulk materials, while it is about 2.044 Å for the surface parts of CTAB-coated Fe_2O_3 nanoparticles, which is obviously larger than the values for the bulk materials and the core part. The CTAB cation ligand tends to bond with the oxygen of the outer shell of the Fe_2O_3 nanoparticle, while the DBS anion ligand tends to attract the Fe cation and compensates for the oxygen vacancy of the outer shell of the Fe_2O_3 nanoparticle. Obviously, the cation surfactant (CTAB) makes the thickness of the surface, the bond length, and the anharmonicity larger; it has more influence than the anion surfactant (DBS) on the atomic structure of Fe_2O_3 nanoparticles.

Acknowledgments

Wu Zhonghua is indebted to the foundations for returning scholars of the Chinese Academy of Science and Chinese Ministry of Education. Guo Lin is grateful to the postdoctoral foundation of the Chinese Academy of Sciences, and the doctoral programme of the Institute of High Education of China (No 95968). The authors are grateful to the anonymous referees for their reviewing of this paper.

References

[1] Music S, Czako-Nagy I, Salaj-Obelic I and Ljubesic N 1997 *Mater. Lett.* **32** 301
[2] Vollath D, Szabo D V, Taylor R D and Willis J O 1997 *J. Mater. Res.* **12** 2175
[3] Peng J and Chai C C 1993 *Sensors Actuators* B **13–14** 591
[4] Peng Y Q, Wang T, Zou S Y, Bu W and Zheng L D 1994 *Acta Phys. Sin.* **43** 1208
[5] Fei H S, Gao M Y, Ai X C, Yang Y Q, Zhang T Q and Shen J C 1996 *Appl. Phys.* A **62** 525
[6] Bodker F, Morup S and Linderoth S 1994 *Phys. Rev. Lett.* **72** 282
[7] Ai X C, Fei H S and Yang Y Q 1994 *J. Lumin.* **61+62** 364
[8] Ying J Y 1992 *Mater. Lett.* **15** 180
[9] Kubo R 1962 *J. Phys. Soc. Japan* **17** 986
[10] Ozaki M, Kratohvil S and Matijevic E 1993 *J. Colloid Surf.* A **70** 167

[11] Kandori K, Tamura S and Ishikawa T 1994 *Colloid Polym. Sci.* **272** 812
[12] Gao M Y, Peng X G and Shen J C 1994 *Thin Solid Films* **248** 106
[13] Sayers D E and Bunker B A 1988 *X-Ray Absorption: Principle, Applications and Techniques of EXAFS, SEXAFS and XANES* ed D C Koningsberger and R Prins (New York: Wiley) ch 6, p 221
[14] Bunker G 1983 *Nucl. Instrum. Methods* **207** 437
[15] Tranquada J M and Ingalls R 1983 *Phys. Rev.* B **28** 3520
[16] Marezio M and Dernier P D 1971 *Mater. Res. Bull.* **6** 23
[17] Lu K Q and Wan J 1987 *Phys. Rev.* B **35** 4497
[18] Lytle F W, Sayers D E and Stern E A 1989 *Physica* B **158** 701